SULPHUR INDUCED CHANGES IN THE BAND GAP ENERGY AND THE TRANSPARENCY WINDOW OF CHEMICAL BATH DEPOSITED ZnO:S THIN FILMS

R. CHIKWENZE[a*], S. EZUGWU[b]

[a]Dept. of Physics/Geology/Geophysics, Federal University, Ndufu Alike, Ikwo Nigeria.
[b]Dept. of Physics & Astronomy, University of Western Ontario, London, ON, N6A 3K7, Canada

We report the enhancement of optical properties, close to infrared spectral region in ZnO thin films by incorporating a sulphur precursor during the films growth process. The deposition of ZnO:S thin film was carried out by chemical bath technique. $Zn(NO_3)_2$ was used as source of zinc ion, $SC(NH_2)_2$, as the source of sulphur ions while ammonium solution served as the complexing agent. Optical properties were studied extensively in the wavelength range of 300-1100 nm. From the measured transmission spectra, the direct band gap energy was determined and found in the range of 3.0 – 3.8 eV. The results show that the beneficial effect of thermal annealing on ZnO:S thin films is quite limited. Instead, the inclusion of sulphur enhances the optical transparency of the film in the NIR region to above 70%.
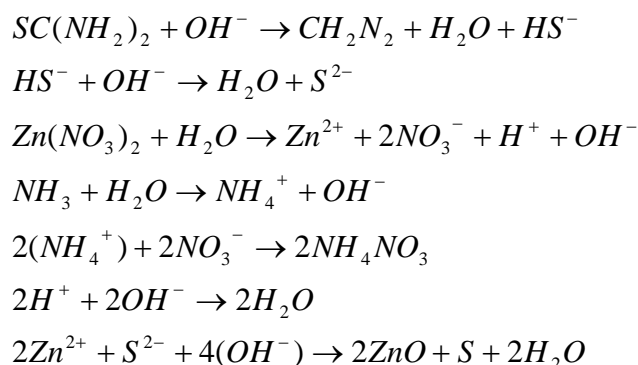
1. Introduction

High quality ZnO thin films are large band gap material which is both transparent and semiconducting [1-4]. In our earlier work, we showed that the band gap energy can be tuned by controlling the deposition parameters during the film growth processes, which was achieved by chemical bath deposition technique [5, 6] and aqueous chemical growth method [7]. In particular, we showed that the pH of the deposition bath [5], film growth time [7], annealing condition and deposition medium [6], can change the optical properties and band gap energy of ZnO thin films. The films were shown to be transmitting almost equally in all the wavelength range studied. Since ZnO is a suitable material for use in solar cells [8, 9], especially as a window layer in thin film solar cells [10, 11] and as transparent electrodes for solar cells[12], it is desirable to tune and increase the spectral response of the film in the visible as well as the NIR region. This is especially important when a photoactive semiconductor for use in optoelectronic devices is poorly absorbing in the long wavelength range.

This paper therefore focuses on the possibility of enhancing the optical properties of ZnO thin film by doping with sulphur during the film preparative stage achieved only by chemical bath deposition. Therefore, by this technique, we extend our capability to control the optical properties of solution prepared ZnO thin films. We show that the transparency window of ZnO films can be increased further in the NIR region of the solar spectrum with a reduction in the reflectance of the film in the visible and NIR, through the incorporation of a sulphur precursor during the films growth process, while retaining the large band gap energy associated with the un-doped film.

---

*Corresponding author: racychikwe@gmail.com

2. Material and methods

The preparation of ZnO:S thin films on glass slide was carried out using chemical bath deposition technique. Prior to the deposition, glass microscope slides were cleaned by degreasing them in dilute hydrochloric acid for 2 hours, washed in detergent solution, rinsed in distilled water and dried in oven at 30°C above room temperature. The starting solution for the deposition of ZnO:S thin films contains 0.5M of $Zn(NO_3)_2$ (zinc nitrate), which acts as the principal precursor solution, 0.1M of $SC(NH_2)_2$ (thiourea), while ammonia solution (NH_4OH) was added to maintain the pH value of the bath at 9.8. NH_4OH also acts as the complexing agent that initiates the formation of complex ions in solution. The molarity of the precursors, as stated above is the optimized values that gave the best result. In a particular deposition set up, equal volume of the precursors were carefully measured into clean 100 ml beaker to form a deposition bath of 80 ml solution. Distilled water has been added to each of the solutions prior to the formation of the solution bath. The mixture was gently stirred for few minutes to ensure good homogeneity of the resulting solution. The reactions taking place in the chemical bath can be summarized as follows:

$$SC(NH_2)_2 + OH^- \rightarrow CH_2N_2 + H_2O + HS^-$$

$$HS^- + OH^- \rightarrow H_2O + S^{2-}$$

$$Zn(NO_3)_2 + H_2O \rightarrow Zn^{2+} + 2NO_3^- + H^+ + OH^-$$

$$NH_3 + H_2O \rightarrow NH_4^+ + OH^-$$

$$2(NH_4^+) + 2NO_3^- \rightarrow 2NH_4NO_3$$

$$2H^+ + 2OH^- \rightarrow 2H_2O$$

$$2Zn^{2+} + S^{2-} + 4(OH^-) \rightarrow 2ZnO + S + 2H_2O$$

In the deposition bath, the ZnO film and the S atom are deposited heterogeneously on the glass slide. In the process, S atom is doping the ZnO through specific O substitution, which results to a matrix semiconductor thin film composed of ZnO:S. Three microslides were inserted into the solution bath through a synthetic form cover and the deposition was allowed to proceed for 4 hours in the oven maintained at 65°C. The deposited films were uniform, after flushing with a fountain of distilled water. Two of the films were annealed at temperatures higher than the deposition temperature. The films were then stored for characterization.

Optical properties of chemical bath deposited ZnO:S thin films were measured at room temperature using Unico – UV-2102PC spectrophotometer at normal incident of light in the wavelength range of 200-1000 nm. Optical band-gaps of the samples were calculated from the absorption spectra. X-ray diffraction (XRD) was recorded using Philips PW 1500 X-ray diffractometer of CuKα wavelength (1.5408Å) while the composition of the films was determined by using Rutherford back scattering.

3. Results and discussion

3.1 Composition and structural properties
The elemental composition and chemical states of the sample annealed in the oven at 150°C was analyzed by Rutherford Backscattering (RSB) at Centre for Energy Research and Development, Obafemi Awolowo University, Ile-Ife, Nigeria. The result of the RBS shown in Figure 1 is presented in Table 1 for clarity, and gives the ratio of the elements in the film as well as the glass substrate. The thickness of ZnO:S deposited on glass slide as determined from the RBS analysis was ~ 300 nm
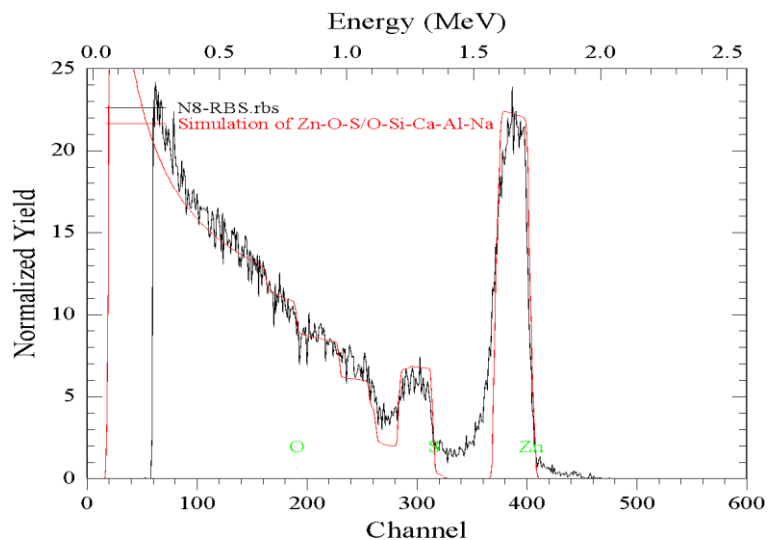
Fig. 1: RBS of ZnO:S thin film annealed at 150ºC

Fig. 2 shows the XRD patterns of ZnO:S thin films deposited in this work. Peak broadening has been observed in recorded diffraction patterns, which shows the formation of crystalline thin films. A close examination of the diffractograms show little improvement in the crystallinity of the films when annealed. However, there is slight broadening of the line with a preferential orientation at 2θ angle of 31.77º and 34.42 that correspond to (100) and (002) planes (JCPDS 36-1451)
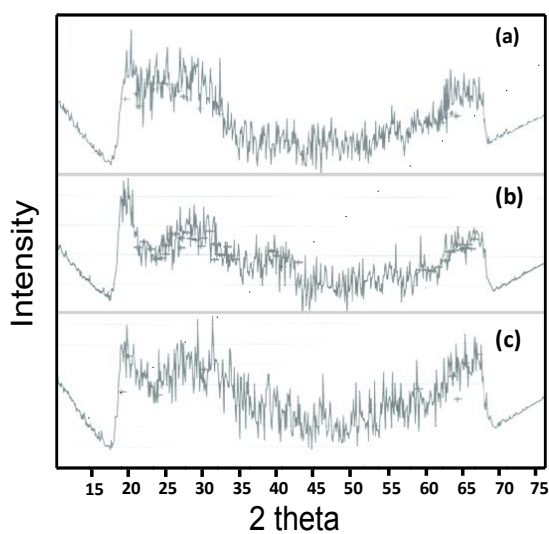

Fig.2. XRD of ZnO:S thin film (a) as-grown (b) annealed at 150ºC and (c) annealed at 250ºC

Table 1. The composition of substrate and ZnO:S film from RBS analysis

	Zinc	Oxygen	Sulphur	Silicon	Calcium	Aluminium	Sodium
ZnO:S thin film	0.440	0.443	0.117	-	-	-	-
Glass substrate	-	0.550	-	0.120	0.050	0.100	0.180

3.2 Optical properties

The transmittance and reflectance spectra of ZnO:S annealed at two different temperatures and the as-grown film is shown in Figure 3. It is observed in panel (a) of Figure 3 that the transmittance decreases with the annealing temperature, signifying possible increase in the density of film and compactness. A beneficial effect of thermal annealing of thin films is the ability to 'heal' porosity and defects. Consequently the film becomes denser and less transmitting. Besides, the inclusion of sulphur in the structure of ZnO has also initiated UV absorption of the incident light waves. Within this spectral region, the optical reflectance of the film is nearly constant irrespective of the annealing condition. This is shown in panel (b) of Figure 3 where it could be seen that the reflectance increases up to a threshold level before decreasing with increasing wavelength.
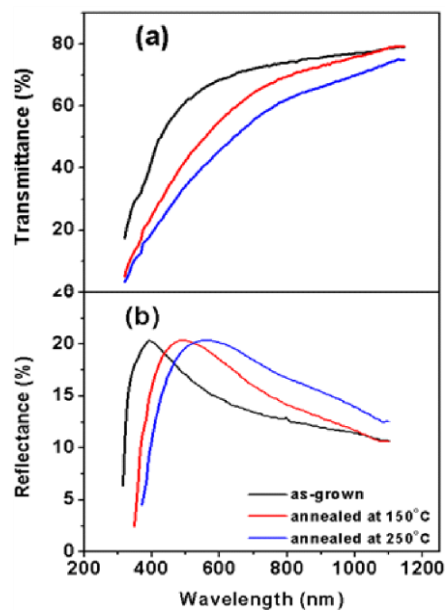

Fig. 3. Plot of (a) spectral transmittance and (b) reflectance of sulphur doped ZnO thin films. Two of the deposited films were annealed at 150°C and 250°C for 1 hour.

The condition of constant reflectance in the UV region corresponds to higher energy absorption seen in Figure 4, which is a plot of the absorption coefficient against the photon energy. The films absorb little in the NIR and slightly higher in the VIS regions of electromagnetic spectrum. The high absorption in the UV region is possibly due to bound state as a result of sulphur dopant. The inclusion of S in ZnO structure has therefore initiated a change in the optical and solid state character of the parent oxide. The film became more transparent to visible and near-infra red electromagnetic waves while depicting strong absorption in the lower spectral region. The selective spectral transmittance and reflectance made possible by sulphur inclusion has an added advantage of expanding the application areas of the films.
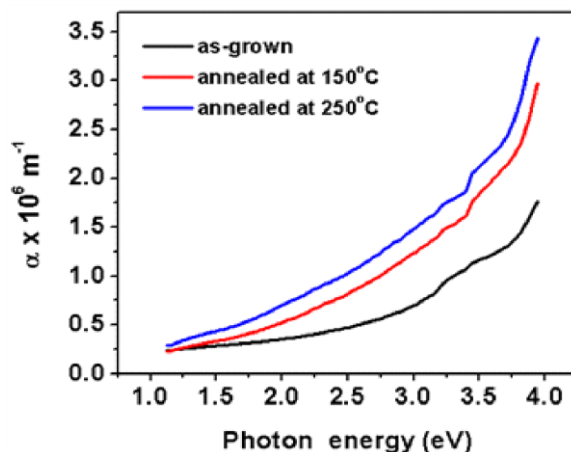
*Fig. 4. Absorption coefficient vs. photon energy for ZnO:S thin films annealed
at two different temperatures and the as-grown film*

The absorption spectra are employed in the determination of the energy gap, E_g. The E_g was calculated using the following relation [13, 14]:

$$\alpha = A(h\nu - E_g)^n / h\upsilon \tag{1}$$

where A is a constant, $h\upsilon$ is the photon energy and α is the absorption coefficient, while n depends on the nature of the transition. For direct transitions $n = \frac{1}{2}$ or $\frac{2}{3}$, while for indirect ones $n = 2$ or 3, depending on whether they are allowed or forbidden, respectively. The best fit of the experimental curve to a band gap semiconductor absorption function was obtained for $n = \frac{1}{2}$.

The calculated values of the direct energy band gap, from Figure 5 are 3.75 eV for the as-grown film and 3.00 eV for the highest annealed film, which gave a band gap shift of 0.75 eV. Annealing the sample in the oven lowers the band gap energy of the film. This observation has been attributed to crystallite size effect, based on the effective mass approximation [15, 16]. So the band gap decreases at higher annealing temperatures as a result of the increase in crystallite size [16].
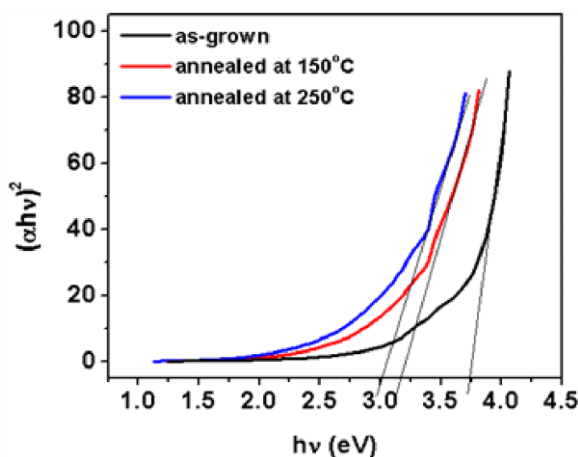

Fig. 5: Plot of direct band gap energy of ZnO:S thin films

The use of thin films in optical applications requires accurate knowledge of optical constants over a wide wavelength range. For instance, the extinction coefficient (k) is related to α by the relation [17, 18]:

$$k = \frac{\alpha \lambda}{4\pi} \tag{2}$$

The reflectivity (R) of materials of refractive index (n) and extinction coefficient (k) is given by [17, 19]:

$$R = \frac{(n-1)^2 + k^2}{(n+1)^2 + k^2} \tag{3}$$

The optical transmittance (T) is related to the absorption coefficient (α) and the refractive index (n) by the relation [18]:

$$T = (1-R)^2 \cdot \exp(-\alpha d) \tag{4}$$

By these relations, k and n can be defined from the measurements of R and T. Once n and k are know, it is straight forward to calculate the dielectric constants via the following two equations:

$$\varepsilon_r = n^2 - k^2 \tag{5}$$

for real part, and

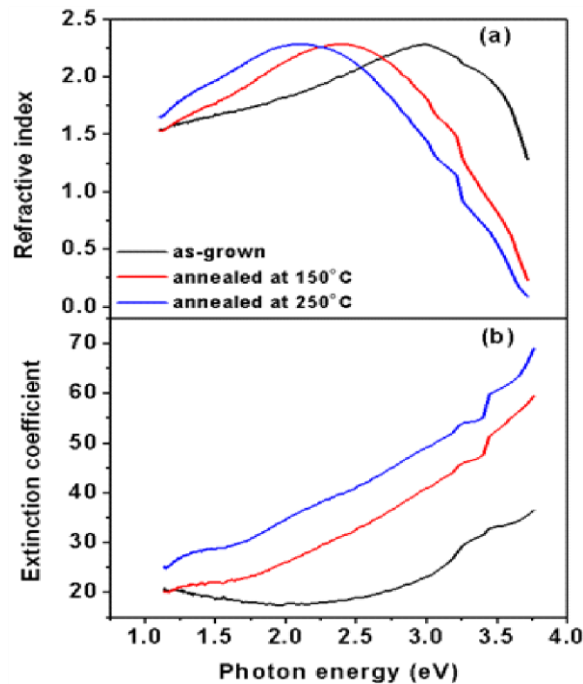$$\varepsilon_i = 2nk \tag{6}$$

for the imaginary part.

Fig. 6: Plot of (a) refractive index and (b) extinction coefficient against photon energy for ZnO:S thin films annealed at two different temperatures and the as-grown film.

The variation of the extinction coefficient k and refractive index with photon energy for the films are shown in Figure 6. It can be observed from Figure 6 that the extinction coefficient increases with both photon energy and annealing temperature. However, the refractive index of ZnO:S thin film increases gradually with photon energy up to a certain value and then begins to decrease. The annealed film has higher values of refractive index up to certain threshold, where it

drops to a value lower than the as-grown film. This threshold corresponds to the wavelength in the range of 496 – 563 nm.

The graph of real and imaginary dielectric constants against photon energy for the ZnO:S thin film is shown in Figure 7. The dielectric constants have similar trend in their values with increasing photon energy. The samples show a gradual increase in the dielectric constant up to certain maximum and then decrease to low values at high photon energy. For the imaginary part of the dielectric constant, the peak value for the as-grown film fall within the UV region and blue shifted with the annealing temperature. In order words, the extinction of electromagnetic waves in the visible region increases with the annealing temperature. The as-grown film has very low extinction coefficient in the visible region, as previously shown in Figure 6(b). Therefore, the as-grown film present better features required for application as window layer in solar cell architecture. This is clearly the case in view of other interesting attributes exhibited by the as-grown sample: higher transmittance in the visible region, large band gap energy as well as low reflectance in the visible. In view of these interesting properties, it can be concluded that the beneficial effect of annealing the films at higher temperatures is limited in this case.
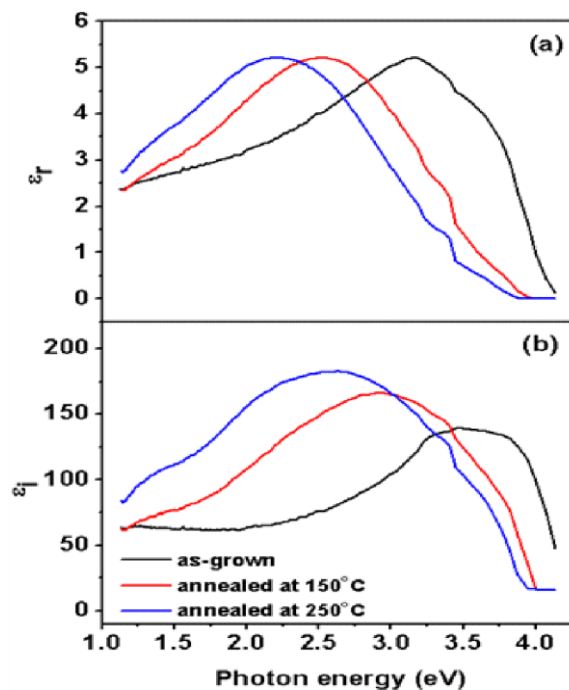

Fig. 7: Plot of (a) real and (b) imaginary dielectric constant against photon energy for ZnO:S thin films annealed at two different temperatures and the as-grown film.

4. Conclusion

ZnO:S thin films were deposited onto glass slides using chemical bath deposition technique. XRD study carried out on the films reveal slightly better crystallization at higher annealing temperature. Through the optical studies and band gap analysis, we demonstrated that high temperature annealing is counter effective in enhancing the optical and solid state properties of ZnO:S thin films. The films exhibit better optical properties suitable for use as window layer in thin film solar cell architecture in its un-annealed form: Large band gap energy and higher transmittance in the visible region. The inclusion of S in the structure of ZnO thin films also moderates the spectral response of the samples, including well defined UV absorption and higher NIR transmittance.

References

[1] S. K. Panda and C. Jacob, Solid-State Electronics **73**, 44 (2012)

[2] A. Janotti and C. G. Van de Walle, Rep. Prog. Phys. **72**, 126501 (2009)

[3] D. C. Reynolds, D. C. Look, B. Jogai, C.W. Litton, G. Cantwell and W.C. Harsch, Phys. Rev. B **60,** 2340 (1999)

[4] X.D. Gao, X.M. Li, W.D. Yu, L. Li, J.J. Qiu and F. Peng, Solar Energy Materials & Solar Cells **91**, 467 (2007)

[5] A. E. Ajuba, S. C. Ezugwu, B. A. Ezekoye, F. I. Ezema and P. U. Asogwa, Journal of Optoelectronics and Biomedical Materials, **2(2),** 73 (2010)

[6] S. U. Offiah, S. C. Ezugwu, F. I. Ezema, O. U Oparaku and P. U. Asogwa, Journal of Ovonic Research, **6(3),** 135 (2010)

[7] S. C. Ezugwu, F. I. Ezema, P. U. Asogwa, A. E. Ajuba, M. P. Ogbu and D.D.O Eya, Digest Journal of Nanomaterials and Biostructures, **6(3),** 1301 (2011)

[8] V. Sittinger, F. Ruske, W. Werner, B. Szyszka, B. Rech, J. Hupkes, G. Schope and H. Stiebig, Thin Solid Films **496**, 16 (2006)

[9] J. Hupkes, B. Rech, S. Calnan, O. Kluth, U. Zastrow, H. Siekmann and M. Wuttig, Thin Solid Films **502**, 286 (2006)

[10] K. Ellimer. 25th IEEE Photovoltaic Specialists Conference, 881 (1996)

[11] Y. Hagiwara, T. Nakada and A. Kunioka. Sol. Energy Mat. & Sol. Cells, **67(1-4)**, 267 (2001)

[12] K. Westermark, H. Rensmo, A.C. Lees, J.G. Vos and H. Siegbahn, Journal of Physical Chemistry B **104**, 319 (2002)

[13] P.U. Asogwa, Chalcogenide Letters, **8(3),** 163 (2011)

[14] J. Tauc, Amorphus and Liquid Semiconductors (New York, Plenum) p. 159 (1974)

[15] S. Erat and H. Metin, Sixth International Conference of the Balkan Physical Union, 249 (2007)

[16] A. Popa, M. Lisca, V. Stancu, M. Buda, E. Pentia, T. Botila, J. Optoelectro. Adv. Mater. **8**(1), 43 (2006)

[17] I.C. Ndukwe, Sol. Ener. Mater. Sol. Cells, **40**, 123 (1996)

[18] J. I. Pankove, Optical Processes in Semiconductors, Prentice-Hall, New York (1971)

[19] M. Janai, D.D. Alfred, D.C. Booth and B.O. Seraphin, Sol. Ener. Mater. **1**, 11(1979)